

Technical note

# Neutron physics analyses of accelerator-driven subcritical assemblies

C.H.M Broeders \*, I. Broeders

*Institute for Nuclear and Energy Technologies, Forschungszentrum Karlsruhe, Postfach 3640, 76021, Karlsruhe, Germany*

Received 14 December 1999; received in revised form 22 March 2000; accepted 18 April 2000

---

## Abstract

In order to improve the safety characteristics of nuclear systems, accelerator driven assemblies have been proposed for energy production and for the incineration of the residuals of the back-end of the nuclear fuel cycle like plutonium, minor actinides and long-lived fission products. For the neutron physics analysis of such source driven systems calculation procedures have been established and qualified at FZK. Necessary extensions to the conventional methods for fission reactors are discussed in some detail, especially for the spallation processes initiated by protons with energies of about 1 GeV. The application of these methods in an IAEA benchmark for an energy amplifier type of ADS identified the problem of the unfavorable power distribution in such sub-critical systems. In order to improve the power distributions the application of multiple sources, radial distributed over the reactor assembly has been proposed. Investigations for an ADS with three proton beams are performed with respect to the capability of incineration of plutonium and minor actinides. © 2000 Elsevier Science B.V. All rights reserved.

---

## 1. Introduction

The use of accelerator-driven subcritical reactors for burning radioactive waste and plutonium and for energy generation is being studied by many research groups (e.g. in the USA, in Japan, and in a number of European countries).

One important reason for this interest is the

possibility to generate fission energy and, at the same time, burn radioactive waste with these reactor systems. A decisive advantage of accelerator-driven subcritical reactors is expected to be the absence of energetic reactivity accidents (of the type occurring, e.g. in Chernobyl) provided that sufficient subcriticality is ensured.

Work in many laboratories has resulted in a variety of concepts of such hybrid systems, and the development of new technical variants is not yet over.

Thus, a technology was elaborated within the ADTT (Accelerator Driven Transmutation Tech-

---

\* Corresponding author. Tel.: +49-7247-822484; fax: +49-7247-823824.

*E-mail addresses:* cornelis.broeders@iket.fzk.de (C.H.M. Broeders), irmgard.broeders@iket.fzk.de (I. Broeders).

nology) project in Los Alamos, USA under the leadership of C.D. Bowman (Bowman et al., 1992) in which radioactive waste is dissolved in a molten salt solution. The molten salt solution is piped through a moderator (e.g. graphite) arranged around the neutron-producing target (spallation target) and, in turn, surrounded by a reactor pressure vessel. The neutrons, which are thermalized by scattering in the moderator, reach a very high neutron flux density and hit the actinides and fission products of the radioactive waste, which are transmuted (burned) by fission or neutron capture (Jameson et al., 1995; Bowman and Newman, 1996). As a consequence of the high thermal neutron flux density and the high cross sections for thermal neutrons, incineration is achieved in a relatively short period of time (within hours or a few days).

In Europe, C. Rubbia and co-workers published two studies in late 1995 (Rubbia et al., 1995a,b), in which accelerator-driven subcritical reactors with solid fuel and a fast neutron spectrum are examined. The fuel of these assemblies is based on thorium. Thorium instead of uranium as a basic fuel offers the advantage of the burning process generating very little plutonium and higher actinides (Am, Cm...).

The power of such a hybrid system is regulated via the proton current intensity of the accelerator. This must be the higher, the more reactor power is to be achieved. Moreover, the required proton current intensity is the higher, the further the reactor deviates from criticality ( $k_{\text{eff}} = 1$ ). The power,  $L$ , of the reactor is approximately directly proportional to the proton current intensity,  $I$ , and inversely proportional to  $(1 - k_{\text{eff}})$ :  $L \sim I/(1 - k_{\text{eff}})$ . Studies by Rubbia and co-workers have indicated that the hybrid systems they examined (Rubbia et al., 1995a,b) require for a reactor power of 1500 MWth an accelerator which is able to accelerate protons to 1 GeV (1000 MeV) and generate a proton current intensity of 10–20 mA. Even higher proton current intensities are needed in the designs of other groups.

Fig. 1, which was taken from (Rubbia et al., 1995a), shows the basic design of such a subcritical system driven by an accelerator. The high-energy protons hit the spallation target (which may

be made of liquid lead) and generate some 20–40 neutrons per proton. The neutrons lose part of their kinetic energy in the target and in the subsequent ‘buffer zone’, which may also consist of lead, before they enter the fuel and blanket material region where they cause nuclear fissions and, hence initiate the production of more neutrons.

In the former Institute for Neutron Physics and Reactor Technologies (INR)<sup>1</sup> code systems were developed in order to assess the neutron physics of existing concepts and to perform neutron physics calculations. These codes describe the neutron processes in a large energy range, from the generation of the neutron source from high-energy protons till the burn-up characteristics of the reactor.

## 2. Calculation methods for accelerator-driven subcritical reactors

Neutron physics calculations for critical reactors, and also for subcritical reactors with external neutron sources, have been carried out at INR for

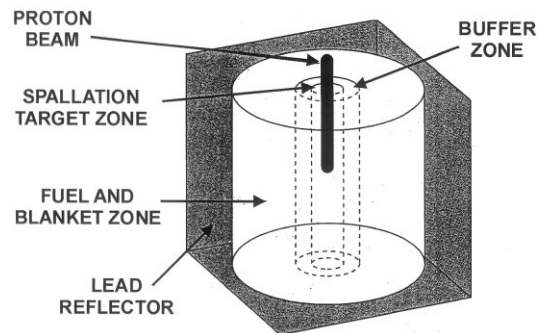


Fig. 1. Basic design of an accelerator-driven subcritical system, cf. (Rubbia et al., 1995a). A high-energy proton beam (e.g. with a radius of 10 cm) hits a target. Spallation reactions cause neutrons to be knocked out of the target which lose part of their kinetic energy in the target and the buffer zones (as a result of further spallations or in scattering processes) before they enter the fuel and blanket zones where they contribute to maintaining the chain reaction in the subcritical reactor by fission reactions.

<sup>1</sup> Since April 1999 part of the former Institute for Neutron Physics and Reactor Technologies, INR, belongs to the new Institute for Nuclear and Energy Technologies, IKET.

a long time. This is true for reactors both with fast and with thermal neutron spectra. However, when starting the work on accelerator-driven subcritical reactors, external codes had to be adopted for the calculation of the spallation neutron source.

### 2.1. Calculation of the spallation neutron source

The HETC (High Energy Transport Code) developed at Oak Ridge (Armstrong and Chandler, 1972) is widely used to calculate the spallation neutron source. Many laboratories employ local versions of the code. INR started neutron physics investigations of accelerator-driven subcritical systems at the end of 1991. After some years of experience with the HETC-version modified by the Jülich Research Center (HETC-KFA-2) (Cloth et al., 1988) now mainly the Los Alamos version (LAHET) (Prael and Lichtenstein, 1989) is used. One of the reasons for this choice is that LAHET offers more options for the specification of the proton source, e.g. parallel proton beam with elliptical or rectangular cross section.

In HETC, a Monte Carlo method is used to simulate the interaction of high-energy protons with the nuclei of the target. In the nuclear reaction model used, the proton interacts with single nucleons of the nucleus. In elastic nucleon–nucleon scattering, the proton transmits part of its kinetic energy to one nucleon of the nucleus which, in turn, can transfer part of this energy to another one or leave the nucleus. Besides the elastic processes, there are also inelastic nucleon–nucleon reactions at these high energies, in which  $\pi$ -mesons are produced, e.g. in the  $n + p \rightarrow n + p + \pi^0$  reaction.

At the end of this intranuclear cascade (see Fig. 2), there are a number of nucleons (neutrons and protons) and  $\pi$ -mesons outside the nucleus as well as an energetically excited compound nucleus with a reduced number of neutrons and protons (Cloth et al., 1988) and (Musiol et al., 1988). This excited compound nucleus is able to split and, normally, generate two fission products and two or three neutrons, or emit (evaporate) nucleons and heavier particles (deuterium, tritium,  $\text{He}^3$  and  $\alpha$ -particles). The LAHET code also allows

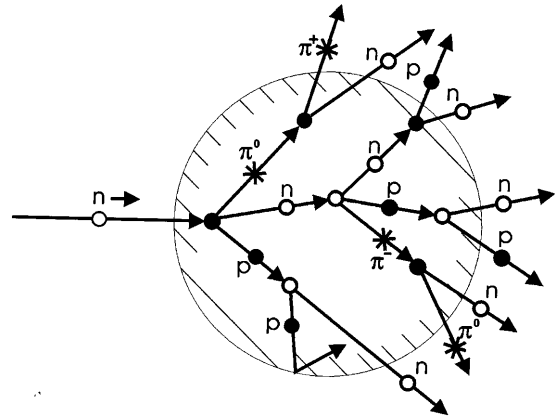


Fig. 2. Schematic representation of an intranuclear cascade when a high-energy neutron hits a nucleus, from (Musiol et al., 1988). In this example, the neutron hits a proton of the nucleus, which may lead to the  $n + p \rightarrow n + p + \pi^0$  reaction. The intranuclear cascade caused by this reaction and the consecutive reactions as well as the reactions with other nuclei are calculated by the Monte Carlo method in the HETC and LAHET codes.

pre-equilibrium processes to be considered after the intranuclear cascade. The nucleons leaving the nucleus during the intranuclear cascade or in the following processes may hit a different nucleus and interact with its nucleons.

The cross sections of the nucleon–nucleon and nucleon– $\pi$ -meson interactions are stored in a library which is part of the code. This library also contains data about the nucleon density and about the kinetic energy per nucleon calculated from the Fermi gas model. In addition to the distributions of energy, position and angle of the neutrons, HETC also computes the distribution of the remaining residual nuclei (spallation products) as a function of the mass number and atomic number. The code also allows other quantities for evaluation to be computed, such as neutron fluxes, heat generation, gas production.

Some results of a calculation with LAHET are shown in Fig. 3 and Fig. 4. In the calculation, a proton beam of 1 GeV impinges upon a cylindrical lead target in the center of a subcritical reactor. For the proton beam, a circular cross section with a radius of 10 cm and a parabolic profile were assumed.

Fig. 3 shows the energy distribution of the spallation neutrons in a cylindrical target of 10 cm radius and 50 cm height in a sub-critical assembly. Most neutrons (16 out of a total of 22.3 neutrons per proton) are produced by evaporation from the excited compound nucleus or by fission of the compound nucleus. Neutrons with energies above 20 MeV are generated mainly in the intranuclear cascade. The mass distribution of the residual nuclei (spallation products) in the target is shown in Fig. 4.

## 2.2. ADS steady state and burnup calculations

The reaction models employed in HETC can no longer be used for neutrons with energies below  $\sim 20$  MeV. Neutrons with energy below a lower limit specified by input (mostly 20 MeV) are written on an interface file in HETC and transferred as external sources to neutron flux calculation codes, such as TWODANT (Alcouffe et al., 1986) (deterministic transport approximation), D3D (Stehle, 1991) (deterministic diffusion ap-

proximation) or MCNP (Briesmeister, 1997) (Monte Carlo transport method). Fig. 5 shows a simplified flow diagram for the neutron physics calculation of an accelerator-driven subcritical reactor.

The codes LAHET and MCNP and auxiliary programs are combined in the LAHET Code System (LCS) (Prael and Lichtenstein, 1989). LCS still requires separate input files for LAHET and MCNP and transfers large data files from one code to the other. Currently MCNPX is being developed at Los Alamos (Hughes et al., 1997). MCNPX is a merge of LAHET and MCNP. It needs only one input file for both codes and partly avoids the transfer of large data files.

The energy range between  $10^{-5}$  eV and 20 MeV is covered in extensive nuclear data libraries evaluated and continuously updated on an international level, such as ENDF, JEF, EFF. These libraries are being developed mainly for calculations of fission and fusion reactors. There have been some recent projects aimed at extending these nuclear data libraries to a neutron en-

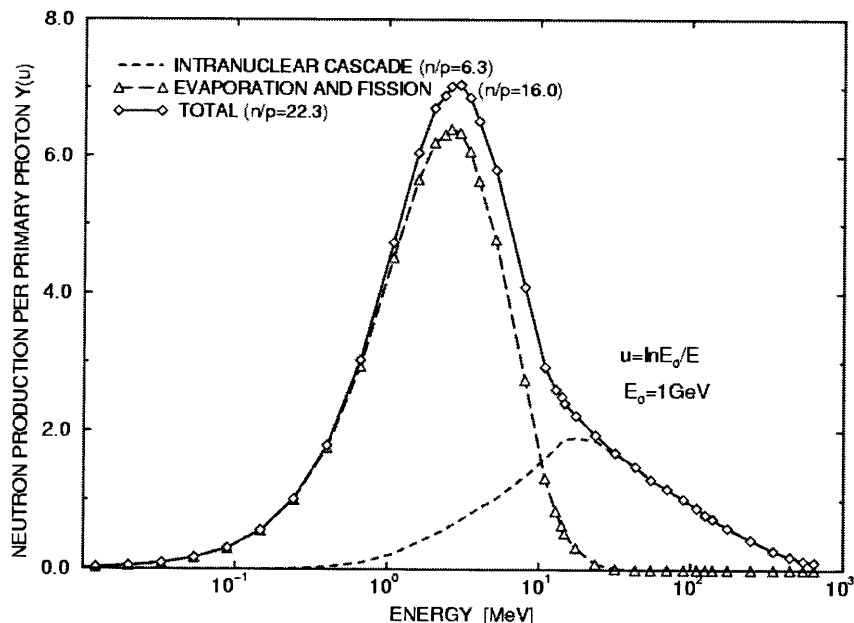


Fig. 3. Energy distribution of the spallation neutrons when a proton beam of 1 GeV hits a Pb target of 10 cm radius and 50 cm height in a subcritical assembly. (The  $n/p$  parameter describes the number of neutrons produced in each case per incident proton.) Most neutrons are emitted by evaporation from the residual nucleus or by high-energy fission of the residual nucleus. The neutrons with energy  $> 20$  MeV mainly come from the intranuclear cascade.

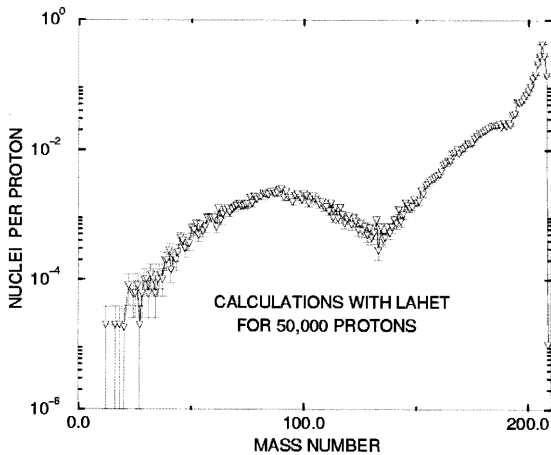


Fig. 4. Mass distribution of the spallation products when a 1 GeV proton beam hits a Pb target. Approximately 2.8 spallation products per incident proton are generated in the Pb target. Their mass numbers are between  $A = 12$  and  $A = 208$ , the maximum being for  $A = 206$ . The figure shows the mean values resulting from the Monte Carlo calculation, and the statistical errors.

ergy of 50 MeV and above (Korovin et al., 1997). The calculations with LAHET for a lead target hit by a 1 GeV proton beam show that

some 86% of the neutrons in the target have an energy below 20 MeV. Some 93% have an energy below 50 MeV, in 96% of the neutrons the energy is below 100 MeV, and for some 98% it is below 150 MeV.

Part of the results obtained with the flux calculation codes, mainly the spatial and the energy distribution of the neutron flux density, are transferred to the KARBUS (Broeders et al., 1992) burnup code in order to determine the change in isotopic composition of the fuel as a function of time, i.e. the burnup of the reactor (see Fig. 5). After a burnup time which can be defined by the code input, and which is usually between some 30 and 150 days, the isotopic composition of the fuel existing at that time is then used for a new calculation of the current neutron distribution.

In principle, these burnup steps may be repeated arbitrarily. There is a possibility to restart after each burnup step (or after several burnup steps) with the fuel composition existing at that time, and to start from calculating the source afresh with HETC/LAHET. This is indicated by the outermost arrow in Fig. 5.

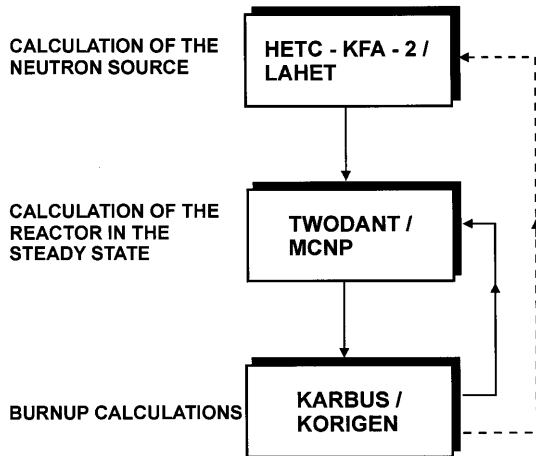


Fig. 5. Schematic layout of the code for a complete neutron physics calculation of an accelerator-driven subcritical reactor. After a burnup time which can be defined by the code input, the neutron flux density spectra are determined repeatedly by TWODANT and MCNP, respectively (inner arrow). There is also a possibility after one or several burnup steps to recalculate the spallation source with HETC and LAHET, respectively (outer arrow).

### 3. Applications

ADS system studies were started as soon as reliable qualified calculation tools were available. After some preliminary studies of the capabilities of ADS for the incineration of plutonium, minor actinides and long lived fission products, see (Broeders et al., 1996), the participation to the IAEA ADS benchmark resulted in insights of large interest. Especially the power distribution towards the central neutron source proved to be unsatisfactory with radial form factors varying from about 2.5 to nearly 4. In order to improve these unacceptable characteristics, at FZK an ADS with up to six distributed neutron sources was proposed and investigated. On the basis of this multi-source design a number of more detailed investigations related to the incineration of plutonium and minor actinides have been performed.

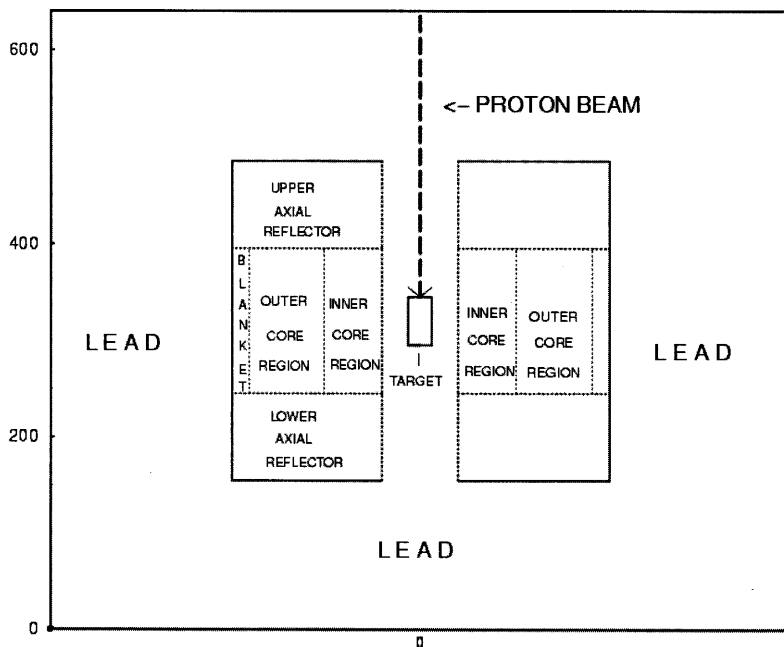


Fig. 6. Longitudinal section through the lead-cooled subcritical reactor defined for the IAEA benchmark exercise with  $\text{Th}^{232}/\text{U}^{233}$  fuel. The target and the buffer zones are made of lead, and the reactor is surrounded by a Pb reflector. The 1 GeV proton beam of 10 cm radius hits the target from the top.

### 3.1. IAEA benchmark for neutron physics calculation of accelerator-driven systems

Groups from Japan, Russia, France, Italy, Switzerland, and Germany participated in a benchmark formulated by IAEA (International Atomic Energy Agency) about the neutron physics calculation of accelerator-driven subcritical systems (Slessarev et al., 1997). The model of the subcritical reactor is based on a proposal by C. Rubbia; a so-called Energy Amplifier (EA). This energy amplifier is a reactor with  $\text{Th}^{232}/\text{U}^{233}$  fuel, with lead as the coolant and moderator and for shielding. Also the target is made of lead. The geometric model of the reactor in principle corresponds to that shown in Fig. 1, but is slightly more complicated. A longitudinal section is shown in Fig. 6.

The target consisting of liquid lead is placed in the center of the reactor and is hit from the top by a 1 GeV proton beam of circular cross section and parabolic profile. The power of the reactor, which

is 1500 MWth, is to be kept as constant as possible over a period of  $\approx 6$  years.

The main purpose of the benchmark was the calculation of criticality ( $k_{\text{eff}}$ ) changes resulting

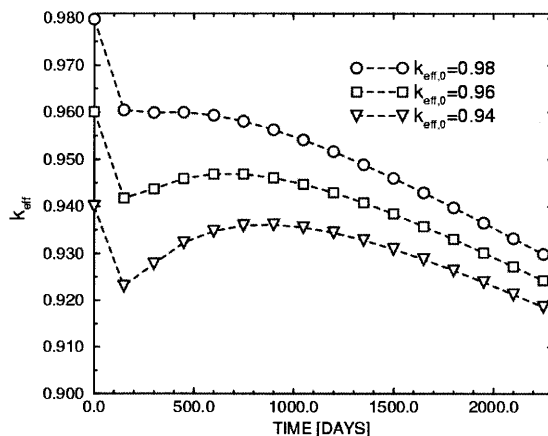


Fig. 7. Behavior of the criticality value,  $k_{\text{eff}}$ , over a burnup period of approximately 6 years for three lead-cooled subcritical reactors with different fuel enrichment levels (and different values of  $k_{\text{eff},0}$ ) in the fresh reactor.

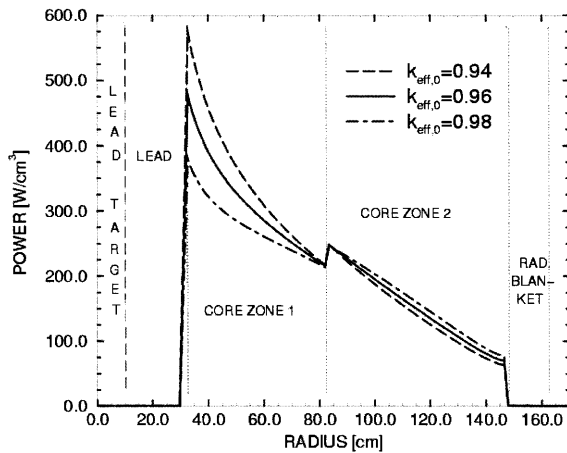


Fig. 8. Radial power distributions for three lead-cooled subcritical reactors with different fuel enrichments. The calculations were performed for the fresh reactors. The results are shown in each case for the core midplane. The strongest radial dependence is found for the reactor with the lowest value of  $k_{\text{eff},0}$ .

from the change in the isotopic composition of the fuel over a period of 6 years (2250 days).

Fig. 7 shows the development of  $k_{\text{eff}}$  as a function of time for three reactors differing in the initial enrichment with  $\text{U}^{233}$  of the fuel and, consequently, having different initial criticality values:  $k_{\text{eff},0} = 0.94$ ,  $k_{\text{eff},0} = 0.96$ , and  $k_{\text{eff},0} = 0.98$ . The diagram shows a pronounced decrease of  $k_{\text{eff}}$  over the first 150 days for all three reactors. The reason is the buildup of  $\text{Pa}^{233}$ , which has a very high neutron capture cross section and, consequently, extracts neutrons from the chain reaction in the reactor. Over the first 150 days,  $\text{U}^{233}$  enrichment in the fuel decreases as a result of fission and neutron capture. Afterwards, the  $\text{U}^{233}$  enrichment increases steadily as a result of the buildup of  $\text{U}^{233}$  from the  $\beta^-$ -decay of  $\text{Pa}^{233}$  with a half-life of 27 days. Consequently,  $k_{\text{eff}}$  rises again after 150 days (see Fig. 7). The decrease of  $k_{\text{eff}}$  after about 900 days is caused by the increase in fission products, some of which are strong neutron absorbers.

Another important objective of the benchmark was the determination of the power distribution in the cores investigated.

Fig. 8 shows the power as a function of the core radius at mid-plane of the reactor for the three cases with different fuel enrichment levels. These

calculations were conducted for the reactors in the fresh state, i.e. for  $k_{\text{eff}} = k_{\text{eff},0}$ . In the target and the buffer zones consisting of lead practically no power is produced; at the inner edge of the core, the power reaches its peak level which (when normalized to the same total power) is the higher, the smaller  $k_{\text{eff},0}$ . For all three enrichment levels, the power decreases very strongly towards the edge of the core. The step increase in power at the boundary from the inner to the outer core zone comes from the slightly higher fuel volume fraction in this outer core zone. The pronounced radial power decrease is typical for subcritical reactors with external neutron sources in the center. In critical reactors, the radial power profile is much flatter, which is favorable for the thermodynamic design and for the burnup behavior of the reactor. The radial power form factors obtained in the IAEA benchmark are not acceptable in large power systems. As a consequence of these observations at FZK a considerable effort was devoted to improve the power-density distribution. Although the typical solution for fast critical reactors to increase the fissile enrichment in two to three radial zones also leads to improvements in an ADS, a better solution seems to be to apply more than one spallation source in the system. Exploratory investigations were carried out for two to six non-central spallation sources. In reference (Dagan and Broeders, 1999) it is shown that a three beam system may probably be a good compromise concerning power density distributions and system complexity. In Fig. 9 an example of a power density distribution in an ADS with  $\text{Th}/\text{U}^{233}$  fuel and three neutron sources is shown. In the next section more detailed information is given for the incineration of plutonium and minor actinides with a three beam ADS.

### 3.2. Plutonium and minor actinide burner

At FZK a main objective of the ADS investigations is to analyze its characteristics for closing the back-end of the nuclear fuel cycle. An important parameter in these studies is the possible incineration rate of plutonium, minor actinides and long-lived fission products. In the next sections two cases for different fuels are presented.

Both cases are based on discharged fuel from pressurized water reactors (PWR) with a mean burn-up of 50 000 MWD/THM. Seven years cooling time and 3 years fabrication time are assumed for the ex-core handling. The investigations are based on a 1500 MWe ADS with lead coolant and 217 hexagonal fuel element positions. The active core height is 150 cm.

### 3.2.1. Incineration in a thorium based system

In a first series of investigations the incineration of a mixture of not-separated heavy metals from spent LWR-fuel with 50 000 MWD/THM mean discharge burn-up was considered. The desired sub-criticality was obtained by mixing this fuel with thorium.

### 3.2.2. Incineration in a thorium- and uranium-free system

In a further series of investigations the incineration of a mixture of separated stocks of plutonium and minor actinides from spent LWR-fuel with 50 000 MWD/THM mean discharge burn-up was considered. The desired sub-criticality was obtained by mixing these fuel components in a

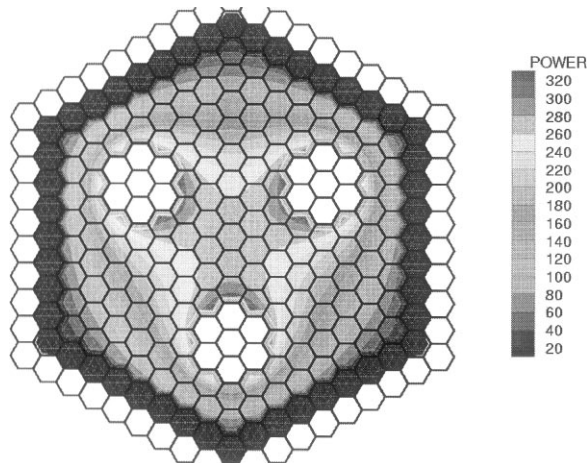


Fig. 9. Power density distribution ( $\text{W}/\text{cm}^3$ ) in a lead-cooled subcritical energy amplifier with  $\text{Th}/\text{U}^{233}$  fuel. The three beams with buffer zones are described by seven lead-filled fuel element positions each. A color scale varies from 20  $\text{W}/\text{cm}^3$  (blue) to 320  $\text{W}/\text{cm}^3$  (red). The power densities have their maximum near the beam buffer zones. The over-all power distribution is satisfactory.

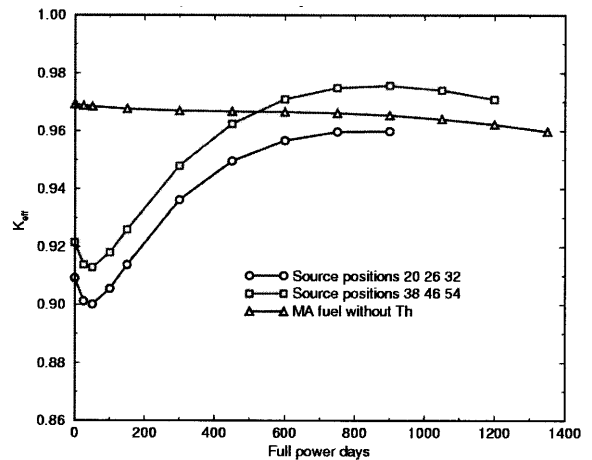


Fig. 10. Burnup dependent criticality of three ADS cores with three proton beams and different fuel compositions. The fuel comes from reprocessed PWR fuel assemblies with 50 000 MWD/THM discharge burn-up. The upper cases utilize a mixture of all reprocessed heavy metals and with thorium. The only difference in these cases is the position of the proton beams. The typical  $\text{Pa}^{233}/\text{U}^{233}$  reactivity swing may be observed. The third case utilizes a mixture of separate stocks of reprocessed plutonium and minor actinides, diluted by zirconium. The result is a flat criticality curve.

proper way and with about 60% zirconium as matrix material.

### 3.2.3. Results

In Fig. 10 the burn-up dependence of the reactivity of the systems described before is shown. The burn-up calculations were terminated after exceeding 140 MWD/THM in any of the reactor zones. For the  $\text{Th}/\text{Pu}-\text{MA}$  fuel two different arrangements of the proton sources are investigated, identified by the fuel assembly numbers (20, 26, 32) and (38, 46, 54). Obviously, the second case with proton sources somewhat more to the outer boundary of the core is more favorable: the reactivity is slightly higher and the upper limit of the fuel burn-up is reached later, indicating better power density distributions.

The  $\text{Th}/\text{Pu}-\text{MA}$  results also show the strong influence of the build-up of  $\text{U}^{233}$  from  $\text{Th}^{232}$  capture with a reactivity increase of about 6% during burn-up. The typical reactivity decrease due to the  $\text{Pa}^{233}$  build-up during the first 50–150 days also may be observed. On the other hand, the  $\text{Th}$ -free

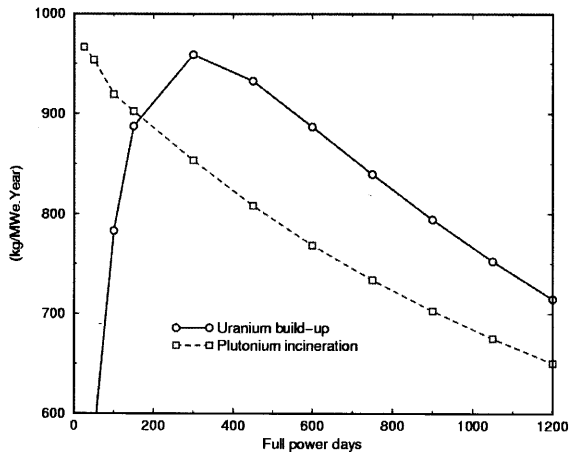


Fig. 11. Comparison of the plutonium incineration and the uranium build-up in an ADS with three proton beams and a fuel mixture of heavy metals from PWR assemblies with 50 000 MWD/THM discharge burnup, mixed with thorium.

fuel leads to a very flat reactivity behavior. In Fig. 11 the change rates in (kg/MWe·Year) of uranium and plutonium in the Th/Pu-MA system are shown. For the normalization to (MWe·Year) a load-factor of 1 and a system-efficiency of 40% are assumed. It may be observed that in this

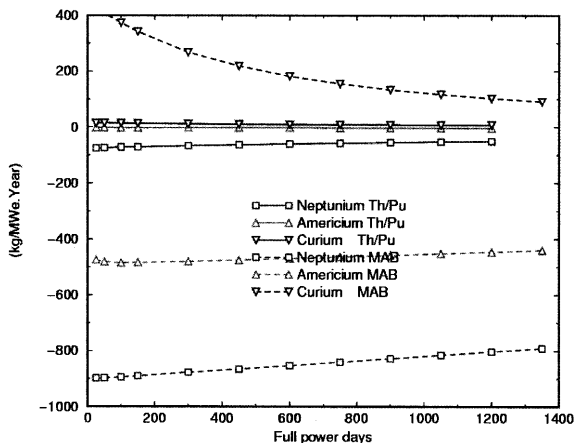


Fig. 12. Comparison of change rates in an ADS with three proton beams and different fuels. In the case of fuel with admixed thorium only small minor actinide change rates may be observed. A remarkable improvement shows the thorium-free fuel (MAB). In these systems the curium amounts always increase (positive change rate).

design the uranium production exceeds the plutonium incineration.

The change rates for minor actinides are given in Fig. 12 for both cases. They are small in the Th/Pu-MA system. In the minor actinide burner system (MAB) the incineration rates of americium and neptunium are much better. Curium is always produced (changes are always positive).

#### 4. Summary and outlook

Accelerator driven subcritical reactor systems (ADS) have been proposed both for energy production and for the incineration of the long-lived isotopes of the back-end of the nuclear fuel cycle. The option to operate at sufficiently low criticality levels to avoid accidents with super-criticality improves the over-all safety of a reactor system. On the other hand the coupling of powerful proton accelerators with large power-generating nuclear reactor systems strongly increases the complexity of the installation. Moreover, the realization of proton accelerators with proton energies around 1 GeV and steady state currents larger than about 10 mA is not yet proven technology. At present a tendency may be observed to utilize ADS for special problems of the back-end of the nuclear fuel cycle with nuclear fuels not useable in critical reactors due to unfavorable safety characteristics like Doppler effect, coolant density reactivity effect, fraction of delayed neutrons etc.; the so-called double strata concept (see, e.g. reference (Broeders et al., 2000) in this volume).

From the point of view of the neutron physics, the treatment of the coupling of sub-critical reactor systems with powerful proton accelerators is a challenging task. The coupling of spallation target physics and fission reactor physics has to be qualified very carefully. Further, the strong dependence of the power distribution of the level of sub-criticality and the presence of an external neutron source seem to necessitate a review of a number of calculation procedures, especially for the analysis of system transients and system safety (Broeders, 1998).

## References

- Alcouffe, R.E., Brinkley, F.W., Marr, D.R., O'Dell, 1986. LA-10049-M, Revision 1.3.
- Armstrong, T.W., Chandler, K.C., 1972. ORNL-4744.
- Bowman, C.D., Arthur, E.D., Lisowski, P.W., Lawrence, G.P., Jensen, R.J., Anderson, J.L., Blind, B., Cappiello, M., Davidson, J.W., England, T.R., Engel, L.N., Haight, R.C., Hughes, H.G., Ireland, J.R., Krakowski, R.A., La-Bauve, R.J., Letellier, B.C., Perry, R.T., Russel, G.J., Staudhammer, K.P., Versamis, G., Wilson, W.B., 1992. Nuclear Instruments and Methods in Physics Research A320, 336–367.
- Bowman, C.D., Newman B.E., 1996. ICENES'96, Obninsk, Russia, June 24–28.
- Briesmeister, J.F. (ed), 1997. LA-UR-12625-M, Version 4B, issued March 1997.
- Broeders, C.H.M., KfK 5072, August 1992.
- Broeders, I., Broeders, C.H.M., 1996. ICENES'96, Obninsk, Russia, June 24–28.
- Broeders, C.H.M., 1998. EUR 18898 EN, Mol, Belgium, November 25–27.
- Broeders, C.H.M., Kiefhaber, E., Wiese, H.W., 2000 this volume.
- Cloth, P., Filges, D., Neef, R.D., Sterzenbach, G., Ch. Reul, Armstrong, T.W., Colborn, B.L., Anders, B., Brückmann, H., 1998. Jül-2203, May 1988, ISSN 0366-0885.
- Dagan, R., Broeders, C.H.M., 1999. 20 Conference of Nuclear Societies in Israel.
- Hughes, H.G., Prael, R.E., Little, R.C., 1997. LA-UR-97-4891, April.
- Jameson, R.A., Venneri, F., Bowman, C.D., 1995. Alexander-von-Humboldt-Stiftung, Mitteilungen, AvH-Magazin No 66, December.
- Korovin, A.Yu. Konobeyev, P.E. Pereslavitsev, A.Yu. Stankovsky, Broeders, C., Broeders, I., Fischer, U., Möllendorff, U.v., Wilson, P., Woll, D., 1997. International Conference on Nuclear Data for Science and Technology, Trieste, Italy, May 19–24.
- Musiol, G., Ranft, J., Reif, R., Seeliger, D., 1988. Kern- und Elementarteilchenphysik, VEB Deutscher Verlag der Wissenschaften, Berlin. Lizenzausgabe der VCH Verlagsgesellschaft, D-6940 Weinheim.
- Prael, R.E., Lichtenstein, H., 1989. September, LA-UR-89-3014.
- Rubbia, C., Rubio, J.A., Buono, S., Carminati, F., Fiétier, N., Galvez, J., Gelès, C., Kadi, Y., Klapisch, R., Mandrillon, P., Revol, J.P., Ch. Roche, 1995. CERN/AT/95-44(ET), September.
- Rubbia, C., Buono, S., Gonzalez, E., Kadi, Y., Rubio, J.A. 1995. Cern/AT/95-53(ET), December.
- Slessarev, I., Tchistiakov, A., 1997. IAEA TCM-Meeting, Madrid, 17–19 September.
- Stehle, B. 1991. KfK 4764